Available online at www.sciencedirect.com
ScienceDirect
Neuroscience Letters 414 (2007) 192–196
Neuroscience Letters
www.elsevier.com/locate/neulet

Recognition of the physiological actions of the triphasic EMG pattern by a dynamic recurrent neural network

Guy Cheron [a,b,*], Ana Maria Cebolla [a], Ana Bengoetxea [a], Françoise Leurs [a], Bernard Dan [c]

[a] *Laboratory of Neurophysiology and Movement Biomechanics, Université Libre de Bruxelles, CP 168, 50 Av F Roosevelt, Brussels, Belgium*
[b] *Laboratory of Electrophysiology, Université de Mons-Hainaut, Belgium*
[c] *Department of Neurology, Hopital Universitaire des Enfants reine Fabiola, Université Libre de Bruxelles, Belgium*

Received 15 October 2006; received in revised form 14 December 2006; accepted 14 December 2006

Abstract

Triphasic electromyographic (EMG) patterns with a sequence of activity in agonist (AG1), antagonist (ANT) and again in agonist (AG2) muscles are characteristic of ballistic movements. They have been studied in terms of rectangular pulse-width or pulse-height modulation. In order to take into account the complexity of the EMG signal within the bursts, we used a dynamic recurrent neural network (DRNN) for the identification of this pattern in subjects performing fast elbow flexion movements. Biceps and triceps EMGs were fed to all 35 fully-connected hidden units of the DRNN for mapping onto elbow angular acceleration signals. DRNN training was supervised, involving learning rule adaptations of synaptic weights and time constants of each unit. We demonstrated that the DRNN is able to perfectly reproduce the acceleration profile of the ballistic movements. Then we tested the physiological plausibility of all the networks that reached an error level below 0.001 by selectively increasing the amplitude of each burst of the triphasic pattern and evaluating the effects on the simulated accelerating profile. Nineteen percent of these simulations reproduced the physiological action classically attributed to the 3 EMG bursts: AG1 increase showed an increase of the first accelerating pulse, ANT an increase of the braking pulse and AG2 an increase of the clamping pulse. These networks also recognized the physiological function of the time interval between AG1 and ANT, reproducing the linear relationship between time interval and movement amplitude. This task-dynamics recognition has implications for the development of DRNN as diagnostic tools and prosthetic controllers.

Keywords: Human ballistic movement; Triphasic EMG pattern; Dynamic recurrent neural network

The study of rapid, self-terminated movements has demonstrated a triphasic electromygraphic (EMG) pattern on antagonistic muscles [11,2,13]. This pattern is consistent with a single set of control rules taking into account the specificity of the biomechanical and kinematic constraints of the joint [12]. The major features of this pattern are determined by central commands [4] programmed in advance of movement onset, determining EMG pulse intensities, durations, and latencies [10]. A three-pulse control signal based on a sixth-order nonlinear model [12] has permitted to attribute an action pulse (PA) for the first agonist burst, (AG1), a braking pulse (PB) for the antagonist burst (ANT), and a clamping pulse (PC) for the second agonist burst (AG2). However, the interpretation of the differences in the triphasic EMG patterns in terms of pulse-width or pulse-height modulation of rectangular pulses of motoneuron pool excitation do not take into account the complexity of the EMG signal within the bursts. Moreover, such dedicated models do not reach the performance level of the DRNN and do not permit the use of actual EMG signals, as shown important for optimal prosthetic control [19,17].

In order to address these limitations, we applied a neural network methodology previously developed for mapping EMG to kinematics [1,7]. After the learning phase and whatever the type of movement, such a dynamic recurrent neural network (DRNN) identification offers a dynamic memory which is able to recognize the preferential direction of the physiological action of the studied muscles [1,3]. Here we tested the ability of the DRNN to recognize the triphasic-pulse control of ballistic elbow flexion by mapping triphasic raw EMG patterns to angular acceleration of the elbow. Then, we tested the ability of the DRNN to identify specific PA, PB and PC control [12] and the effect of the time interval between AG1 and ANT in the control of movement amplitude [2].

* Corresponding author at: Laboratory of Neurophysiology and Movement Biomechanics, Université Libre de Bruxelles, CP 168, 50 Av F Roosevelt, Brussels, Belgium. Tel.: +32 26502477.
E-mail address: gcheron@ulb.ac.be (G. Cheron).

0304-3940/$ – see front matter © 2007 Published by Elsevier Ireland Ltd.
doi:10.1016/j.neulet.2006.12.019

Informed consent was obtained from 10 neurologically normal subjects (5 female and 5 males, mean 25.6 ± 4.0 years old). The procedures were approved by the local ethics committee of the University and conformed to the Declaration of Helsinki. They were asked to perform 'as fast as possible' flexion movements of the elbow in the vertical plane. The subjects were seated comfortably at a table. The shoulder was flexed at about 30°. At rest the forearm was horizontally on the table, with the elbow extended to about 150°. In order to study the relationship linking the time interval between AG1 and ANT to movement amplitude, 7 subjects were asked to perform 25 movements achieving different target amplitudes (from 5° to 100°). The 3 other subjects performed only movements around 20° amplitude, which served for the DRNN experiment. Surface EMG of biceps and triceps muscles were recorded using pairs of silver–silver chloride electrodes positioned at the approximate geometrical center of the muscle belly (interelectrode distance of 2.5 cm). Raw EMG signals were amplified (1000×), band-pass filtered (10–2000 Hz). Thereafter, EMG signals were digitized at 2 kHz, full-wave rectified and smoothed by means of a 3rd-order averaging filter (time constant of 20 ms). The movements were recorded and analyzed using the optoelectronic ELITE system (BTS, Milan). This system consists of two CCD-cameras (100 Hz) placed 4 m from the subject and detecting retro-reflective markers attached to the arm (on the shoulder, the elbow, the wrist). Acceleration signals were obtained by digitally twice differentiating position signals using a 5-polynomial approximation. For the three subjects used for the DRNN simulation, two movements were selected on the basis of a clear distinction of the triphasic EMG pattern. Then, these EMG patterns and the related acceleration signals were fed into the DRNN as input and output, respectively. The total duration of the treated file was 1000 ms (150 ms before and 850 ms after movement onset). Fig. 1 illustrates the input–output relationships of the DRNN, symbolized by the central ring. The DRNN is a fully connected network of 35 hidden units taking into account the temporal relationships history between input and output signals. The biceps and triceps EMG signal were sent to all 35 units, which converge to one output unit acting merely as summation unit, providing the angular acceleration of the elbow.

The DRNN is governed by the following equations:

$$T_i \frac{\mathrm{d}y_i}{\mathrm{d}t} = -y_i + F(x_i) + I_\mathrm{i} \tag{1}$$

where $F(\alpha)$ is the squashing function $F(\alpha) = (1 + \mathrm{e}^{-\alpha})^{-1}$, y_i is the state or activation level of unit i, I_i is an external input (or bias), and x_i is given by:

$$x_i = \sum_j w_{ij} y_j \tag{2}$$

which is the propagation equation of the network (x_i is called the total or effective input of the neuron, w_{ij} is the synaptic weight between units i and j). The time constants T_i will act like a relaxation process. It allows a more complex frequential behaviour and improves the non-linearity effect of the sigmoid function [7]. In order to make the temporal behaviour of the network explicit, an error function is defined as:

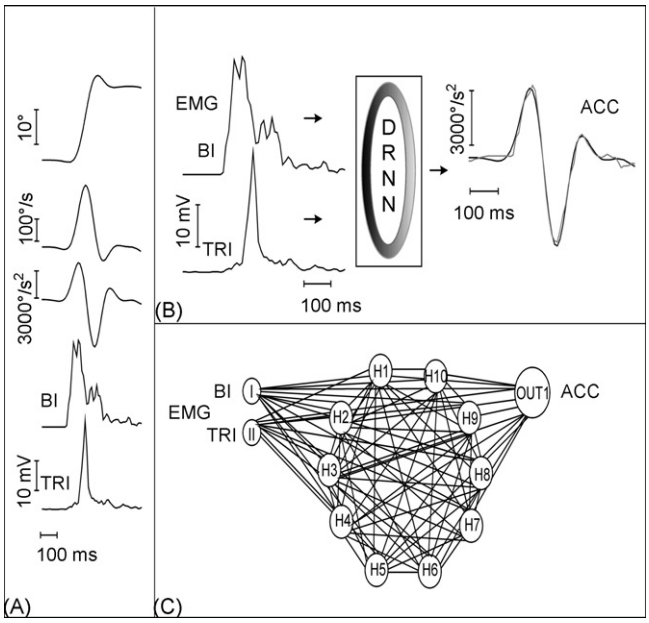

Fig. 1. Input–output configuration of the DRNN. (A) Main characteristics of the ballistic angular movement of the elbow (from top to bottom: angular position, velocity and acceleration, respectively). At the bottom, the triphasic EMG pattern recorded on the biceps (BI) and the triceps (TRI) muscle was represented. (B) Input–output configuration of the DRNN, symbolised by the ring in the central box, with the triphasic pattern as the input and the angular acceleration (ACC) used as output. The experimental (grey) and simulated (black) acceleration curves are superimposed. (C) DRNN fully connected architecture is represented in case of only 13 artificial neurons (10 hidden neurons, H1-H10; 2 input neurons, I and II; and one output neuron, OUT1).

$$E = \int_{t_0}^{t_1} q(y(t), t)\mathrm{d}t \tag{3}$$

where t_0 and t_1 give the time interval during which the correction process occurs. The function $q(y(t), t)$ is the cost function at time t which depends on the vector of the neurone activations y and on time. We then introduce new variables p_i (called adjoint variables) that will be determined by the following system of differential equations:

$$\frac{\mathrm{d}p_i}{\mathrm{d}t} = \frac{1}{T_i} p_i - e_i - \sum_j \frac{1}{T_i} w_{ij} F'(x_j) p_j \tag{4}$$

with boundary conditions $p_i(t_1) = 0$. After the introduction of these new variables, we can derive the learning equations:

$$\frac{\delta E}{\delta w_{ij}} = \frac{1}{T_i} \int_{t_0}^{t_1} y_i F'(x_j) p_j \mathrm{d}t \tag{5}$$

$$\frac{\delta E}{\delta T_i} = \frac{1}{T_i} \int_{t_0}^{t_1} p_i \frac{\mathrm{d}y_i}{\mathrm{d}t} \tag{6}$$

The training is supervised; involving learning rule adaptations of synaptic weights and time constant of each unit [7].

The DRNN was trained to reproduce the ballistic flexion of the elbow. Each training was associated to only one subject and one movement. The error is given by the differential area between the experimental and simulated angular acceleration.

The linear relationship between the AG1-ANT time interval and movement amplitude was verified ($r = 0.9$). In the movement used for DRNN learning, the mean durations of AG1, ANT and AG2 were 98.3 ± 4.0 ms, 83.3 ± 16.3 ms and 101.6 ± 26.3 ms, respectively. The resulting angular movements were characterized by a bell-shaped velocity profile and a triphasic angular acceleration profile (Fig. 1A). The amplitude, the duration and the time to peak of the three acceleration pulses, chronologically referred as ACC1, ACC2 and ACC3 were $3650.4 \pm 494.8°/s^2$, 126.6 ± 8.1 ms, 91.6 ± 9.8 ms; $-5880.5 \pm 1381.6°/s^2$, 106.5 ± 5.1 ms, 48.3 ± 4.0 ms; $2622.9 \pm 1631.6°/s^2$, 88.3 ± 20.4 ms, 31.1 ± 5.7 ms, respectively.

For each selected movement, 30 different training sessions were performed, giving rise to 180 individually trained DRNN. The learning phase was carried out over a maximum of 10000 iterations. One hundred and three (57%) networks reached an error score of (or below) 0.001. We analyzed the physiological plausibility of these networks by applying a selective amplitude increase in each of the 3 EMG pulses.

Increase of PA amplitude produced an increase in ACC1 amplitude, PB an increase in ACC2 and PC an increase in ACC3, indicating independent pulse-height control in 20 (19%) DRNN that had learned successfully. The other learned networks showed more complex identification, which are out of the scope of the present paper. In the DRNN that identified independent pulse-height control, an increase of ACC1 with a logarithmic trend ($r = 0.88$) was obtained when the amplitude of PA was linearly increased (Fig. 2A, black triangles) reaching saturation around an acceleration increase of 80%. ACC2 followed the same trend ($r = -0.80$) (Fig. 2A, black square) when PB was increased reaching saturation at about 60%. In the same way, the increase of PC induced an increase of ACC3 reaching saturation at about 70% (Fig. 2A, black circles). The independence of these EMG bursts from the other accelerating pulses was relatively respected. PA increase had no effect on ACC3 (Fig. 2A, open triangles) and induced a small increase (less than 30%) in ACC2 (Fig. 2A, grey triangles). PB increase had small effects (less than 20%) in ACC1 and ACC3 (Fig. 2A, grey squares and open squares, respectively). PC increase had no effect on ACC1 (Fig. 2, grey circles) and induced a small increase (less than 30%) in ACC2 (Fig. 2A, open circles). This indicates that the functional roles classically attributed to the three EMG bursts of the triphasic pattern in action, braking and clamping [11] were correctly identified by the DRNN.

As timing has also been demonstrated to be crucial for movement accuracy [16], we tested DRNN identification of the temporal structure of the triphasic pattern. Therefore, we introduced an artificial increase in the time interval between AG1 and ANT. Twenty-ms-step (from 20 ms to 60 ms) delays in the onset of ANT relative to AG1 were associated with conservation of the original temporal relationship between AG1 and AG2 (Fig. 3A). Each new temporal EMG configuration was individually fed-in as the input of a DRNN that previously learned mapping of the

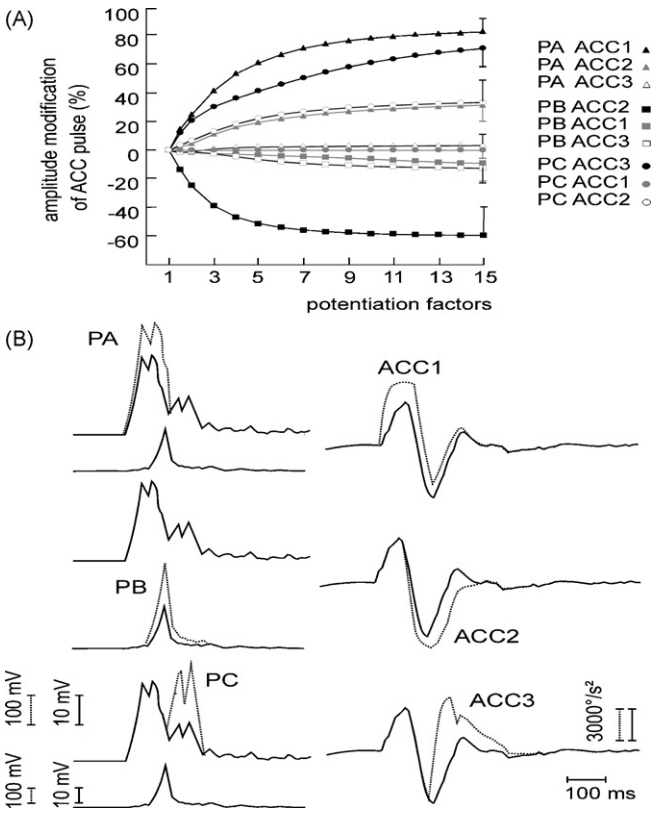

Fig. 2. Simulation of an independent pulse height control on angular acceleration of the elbow. (A) Relationships between the potentiation factors (ranged from 1 to 15) of each single EMG pulse of the triphasic pattern (acting pulse, PA; braking pulse, PB; clamping pulse, PC) and the amplitude of the three different components of the angular acceleration (ACC1, ACC2, ACC3). (B) Examples of independent potentiations of PA (upper traces), PB (middle traces) and PC (lower traces), and their respective effect on ACC1, ACC2 and ACC3, respectively.

original EMG signals onto the actual kinematic output. Without further learning, the DRNN interpreted these modified EMG as producing altered kinematic outputs (Fig. 3A). The main effects of the time shift of ANT onset were reflected in the angular acceleration profile (Table 1). For a 60 ms shift, the duration of ACC1 increased from 126.6 ± 8 ms to 163.3 ± 15 ms, the peak

Table 1
Effect of ANT onset shift on the acceleration pulses configuration

ANT onset shift (ms)	Duration (ms)	Time to peak (ms)	Amplitude (°/s²)
ACC1			
+20	130.2 ± 10.9	73.3 ± 18.6	4021.1 ± 537.8
+40	145.0 ± 20.7	75.7 ± 16.4	4222.7 ± 529.0
+60	163.3 ± 15.0	90.1 ± 29.6	4446.7 ± 477.7
ACC2			
+20	108.2 ± 9.8	43.3 ± 5.1	−5634.2 ± 783.9
+40	233.4 ± 146.1	41.5 ± 7.5	−5623.8 ± 613.6
+60	228.7 ± 137.3	53.3 ± 10.3	−5466.7 ± 302.6
ACC3			
+20	60.1 ± 11.6	26.6 ± 5.1	1588.7 ± 1285.1
+40	32.2 ± 32.8	15.4 ± 16.4	1188.3 ± 1320.5
+60	26.6 ± 29.4	4.1 ± 4.9	380.3 ± 429.3

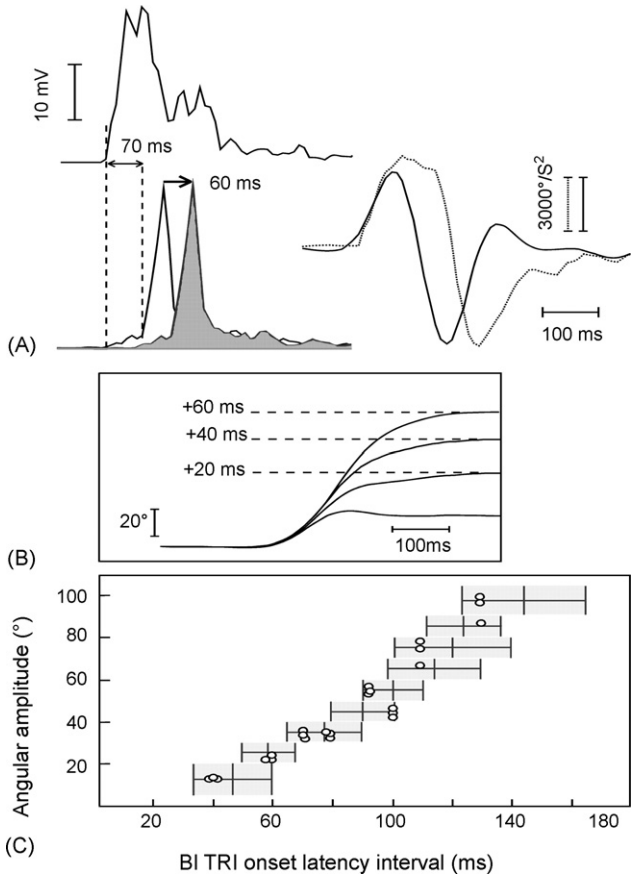

Fig. 3. Simulation of AG1-ANT time interval increase on movement amplitude. (A) example of a time shift of ANT burst (delayed from 60 ms, grey shading of ANT burst superimposed to the experimental pattern). In the left side, the corresponding ACC curves are superimposed (simulated curve in pointed line and experimental curve in continuous line). (B) Progressive increase of angular amplitude when the AG1-ANT interval is increased from 20 ms. C, AG1-ANT time interval and the related movement amplitude. Superimposition of the experimental relationship (the mean and S.D. are represented by the centre and the borders of the grey area, respectively) and the DRNN simulated data (open circles).

of ACC2 was thus delayed and the amplitude of ACC3 was reduced (Table 1). During the progressive shift of ANT burst, the configuration of the angular movement remained roughly the same but with progressively higher amplitude (Fig. 3B). We studied the physiological plausibility of this temporal identification by comparing the experimental relationship between the AG1-ANT time interval and the related ($n = 7$ subjects) and the DRNN simulated relationships ($n = 3$ subjects) (Fig. 3C). The superimposition of the mean ± S.D. values of the experimental data (cross bar in grey area) and the simulated data (open circles) (Fig. 3C) showed that the simulated data fitted well with the experimental linear relationship. Indeed, the simulated points (open circles) are situated inside of the mean ± S.D. area. This demonstrated the physiological plausibility of the DRNN in the identification of the timing of the antagonist burst.

Using artificial learning of the mapping between multiple EMG patterns and elbow angular acceleration we found that the attractor states reached through learning correspond to biologically interpretable solutions. Acceleration signals as DRNN output were used as they present a triphasic configuration, reflecting force control. However, DRNN input consisted only of raw EMG signals, whereas force control does not only depend on muscle activation reflected in the EMG but also on intrinsic properties of contractile apparatus and passive tissue contribution. We used amplification of EMG burst amplitude conserving the physiological complexity of the signal, rather than pulse profile simplification in order to remain closer to the original waveform of the neurophysiological signals that may comprise both reflex and central commands [15]. The central origin of the triphasic EMG burst pattern is consistent with its inclusion in motor strategies, as the ANT burst is not produced when the movement is not self-terminated. The feedforward control of this pattern has been demonstrated by its presence in deafferented patients [9]. Afferent feedback plays a role in fine tuning, mostly when movements include direction changes [18]. The present results demonstrate the ability of the DRNN to recognise the triphasic EMG pattern related to forearm ballistic movement.

Although previous experiments [1,3,7,8] demonstrated DRNN ability to identify the main physiological action of eight different muscles by means of EMG-to-kinematics mapping, the present study shows this ability when EMG input is reduced to two antagonistic muscles. However, only about a fifth of the successful learning trials identified that the amplitude of the accelerating, braking and clamping phases can be modified independently by changing AG1, ANT and AG2, respectively. In the other instances, the DRNN reached alternative dynamic identifications in which the three EMG bursts are interdependent in a complex relationship, whose analysis was out of the scope of the present study. Alternative identification could be due to (1) absence of explicit encoding of anatomy and physiology of muscle acting as eccentric or concentric actuator; (2) only two muscle heads were used in the mapping whereas there are six main actuators involved in the movement; (3) absence of passive contribution of non-muscular elements (e.g. preflex components [5]). The prevalence given here to the independent type of control is motivated by neurophysiological evidence. The cortical control of the triphasic pattern was demonstrated by transcranial magnetic stimulation (TMS) [4,14]. The onset of each single burst can be independently manipulated by ipsilateral motor cortex TMS producing a silent period in the triphasic pattern, demonstrating that the triphasic pattern is not triggered as a single entity, each burst presenting its proper trigger time-window about 30 ms after the start of the preceding burst [14]. This suggests that another part of the motor system is involved in controlling the timing of the bursts. Clinical evidence from cerebellar patients demonstrated that the time interval between AG1 and ANT is one of the main parameters underlying hypermetria, the other parameter being impaired control of ANT amplitude when inertia is increased [16]. These relationships are correctly simulated by the DRNN (Figs. 2 and 3). When the DRNN recognised the independent control of the triple-burst pattern, the artificial increase in the time interval between AG1 and ANT also reproduced the experimental relationship between this agonist–antagonist timing and the related movement ampli-

tude [2]. This result was obtained although the duration of AG1 and the latency of AG2 were not modified, suggesting the prevalence of ANT timing in the control of movement amplitude. This indicates that although only one movement (with a single set of muscle burst amplitude) was used for the training, the DRNN is able to simulate the physiological relationship between EMG burst timing and movement amplitude.

The transformations of the raw EMG signals by kinematics-related data such as those based on Hill's model could improve the identification process [6]. However, contamination of the original neuronal input (raw EMG) by output kinematics-related data (muscle length changes) would bias the spontaneous emergence of multiple attractor states linked to the basic input–output mapping [6]. When the mapping is made between raw EMG signals and kinematics, the distribution of the time constants associated with each neurone-like unit may differ in function of the type of movement, giving rise to tonic and phasic hidden neurones [8]. The present DRNN performance adds to previous identification abilities demonstrated for complex movements such as drawing [1] whole-body straightening [8] and walking [3]. The DRNN identification would probably be improved by increasing the number of recorded muscles including deeper muscles, and by introducing biological EMG filters and sign-adjusted EMG transformation depending of the eccentric or concentric action of the muscle [6]. However, the present DRNN performance including the physiological plausibility of the identification process with only two muscles is advantageous for the control of a prosthetic or orthotic device: (1) on a practical point of view the reduced number of recording electrodes could facilitate the conception of an integrated system and the electrode placement; (2) such a DRNN could produce for each individual subject calibrated ballistic movements without requiring a dedicated muscle model and (3) their physiological plausibility as a triphasic independent pulses control could simplify the final tuning of the based EMG command. Finally, this task-dynamics signal could enhance the performance capabilities of neuroprosthetic controllers for above-elbow amputees.

Acknowledgements

This work was funded by the Belgian Federal Science Policy Office, the European Space Agency (AO-2004, 118), the Belgian National Fund for Scientific Research (F.N.R.S.), the Research Fund of the University of Brussels (U.L.B.). We wish to thank P. Demaret, M. Dufief and E. Hortmanns for expert technical assistance, and S. Labouverie for secretarial assistance.

References

[1] G. Cheron, J.P. Draye, M. Bourgeois, G. Libert, A dynamic neural network identification of electromyography and arm trajectory relationship during complex movements, IEEE Trans. Biomed. Eng. 43 (1996) 552–558.
[2] G. Cheron, E. Godaux, Self-terminated fast movement of the forearm in man: amplitude dependence of the triple burst pattern, J. Biophys. Biom. 10 (1986) 109–117.
[3] G. Cheron, F. Leurs, A. Bengoetxea, J.P. Draye, M. Destree, B. Dan, A dynamic recurrent neural network for multiple muscles electromyographic mapping to elevation angles of the lower limb in human locomotion, J. Neurosci. Methods 30 (2003) 95–104.
[4] B.L. Day, J.C. Rothwell, P.D. Thompson, A. Maertens de Noordhout, K. Nakasashima, K. Shannon, C.D. Marsden, Delay in the execution of voluntary movement by electrical or magnetic brain stimulation in intact man, Brain 112 (1989) 649–663.
[5] M.H. Dickinson, C.T. Farley, R.J. Full, M. Koehl, R. Kram, S. Lehman, How animals move: an integrative view, Science 288 (2000) 100–106.
[6] J.P. Draye, G. Cheron, D. Pavisic, G. Libert, Improved identification of the human shoulder kinematics with muscle biological filters, Lect. Note Ser. Comput. Sci. 1211 (1997) 417–428.
[7] J.P. Draye, D. Pavisic, G. Cheron, G. Libert, Dynamic recurrent neural networks: a dynamical analysis, IEEE Trans. Syst. Man Cybern. 26 (1996) 692–706.
[8] J.P. Draye, J.M. Winters, G. Cheron, Self-selected modular recurrent neural networks with postural and inertial subnetworks applied to complex movements, Biol. Cybern. 87 (2002) 27–39.
[9] R. Forget, Y. Lamarre, Rapid elbow flexion in the absence of proprioceptive and cutaneous feedback, Hum. Neurobiol. 6 (1987) 27–37.
[10] G.L. Gottlieb, A computational model of the simplest motor program, J. Mot. Behav. 25 (1993) 153–161.
[11] B. Hannaford, G. Cheron, L. Stark, Effects of applied vibration on triphasic electromyographic patterns in neurologically ballistic head movements, Exp. Neurol. 88 (1985) 447–460.
[12] B. Hannaford, L. Stark, Roles of the elements of the triphasic control signal, Exp. Neurol. 90 (1985) 619–634.
[13] D.S. Hoffman, P.L. Strick, Step-tracking movements of the wrist in humans. II. EMG analysis, J. Neurosci. 10 (1990) 142–152.
[14] K. Irlbacher, M. Voss, B.U. Meyer, J.C. Rothwell, Influence of ipsilateral transcranial magnetic stimulation on the triphasic EMG-pattern accompanying fast ballistic movements, J. Physiol. (Lond.) 31 (2006).
[15] A.D. Kuo, The relative roles of feedforward and feedback in the control of rhythmic movements, Motor Control 6 (2002) 129–145.
[16] M. Manto, J. Jacquy, J. Hildebrand, E. Godaux, Recovery of hypermetria after a cerebellar stroke occurs as a multistage process, Ann. Neurol. 38 (1995) 437–445.
[17] M.B.I. Raez, M.S. Hussain, F. Mohd-Yasin, Techniques of EMG signal analysis: detection, processing, classification and applications Biol, Proced. Online. 8 (2006) 11–35.
[18] R.L. Sainburg, M.F. Ghilardi, H. Poizner, C. Ghez, Control of limb dynamics in normal subjects and patients without proprioception, J. Neurophysiol. 73 (1995) 820–835.
[19] M. Zecca, S. Micera, M.C. Carrozza, P. Dario, Control of multifunctional prosthetic hands by processing the electromyographic signal, Crit. Rev. Biomed. Eng. 30 (2002) 459–485.